ACS OMEGA

Article

http://pubs.acs.org/journal/acsodf

SiO_2 Fibers by Centrifugal Spinning with Excellent Textural Properties and Water Adsorption Performance

Luděk Hromádko,[†] Eva Koudelková,[‡] Roman Bulánek,[‡] and Jan M. Macak*[,†]

[†]Center of Materials and Nanotechnologies, Faculty of Chemical Technology, University of Pardubice, Nam. Cs. Legii 565, Pardubice 530 02, Czech Republic

[‡]Department of Physical Chemistry, Faculty of Chemical Technology, University of Pardubice, Studentska 573, Pardubice 530 02, Czech Republic

Supporting Information

ABSTRACT: Facile and innovative route for large-scale synthesis of SiO_2 fibers with excellent textural properties and H_2O adsorption performance is presented. At first, a three-dimensional network of SiO_2 precursor fibers was produced from tailored spun solutions (without any toxic elements and surfactants) by centrifugal spinning, which is a very modern fiber-synthesis technique, with numerous advantages over electrospinning. Upon thermal annealing of the precursor fibers, mesoporous amorphous SiO_2 fibers with an ultrahigh surface area of up to 824 m^2/g and pore size distribution in the range of 2−10 nm were produced. Owing to the high number of OH groups available on the surface, the produced SiO_2 fibers showed significantly better performance in H_2O adsorption compared to that of the reference silicagel.

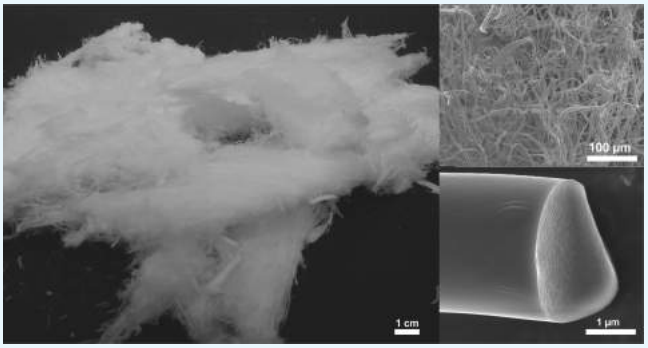

INTRODUCTION

Fibrous structures have been extensively used for decades in various filtration applications, catalysis, health care, textile, etc. Within past 15 years, however, fibers with diameter on the nanometers and sub-micrometers scale have attracted significant scientific and technological attention due to their very high porosity and permeability, often combined with a high specific surface area.[1−3] There are essentially four classes of fibers (including nanofibers) on the basis of their composition: polymeric,[4,5] metal oxide,[6,7] metal,[8] and hybrid ones.[9,10] In particular, nanofibers and microfibers of amorphous SiO_2 have already shown a potential for capturing air moisture,[11,12] as catalyst carriers,[13] or part of solid-state electrolytes of batteries.[14] The specific chemical, electronic, and ionic properties of SiO_2 in combination with high specific surface and three-dimensional (3D) structure of fibers make fibrous materials highly promising for many other applications. In general, numerous techniques for production of nanofibers and microfibers exist, including electrostatic spinning,[15,16] centrifugal spinning,[17,18] pressurized spinning,[19,20] template growth,[21] self-assembly,[22] phase separation,[23] melt-blowing.[24] Nevertheless, the most widely employed technique for these types of fibers has been the electrostatic spinning, known also as "electrospinning", which is based on application of an electrostatic field between the spinnerette (continuously fed with spun solution) and the collecting electrode and consequent withdrawal of tiny fibers from the spun solution toward the collecting electrode.

For an efficient electrospinning process, the first key step is the preparation of stable spun solution. There are many different compositions of spun solutions published in the literature for specific types of fibers. In particular, for SiO_2 fiber synthesis, spinning solutions usually contain a precursor of SiO_2, carrying polymer, solvent, and frequently also additional stabilizers. In most of the published papers, tetraethyl orthosilicate (TEOS) was used as the SiO_2 precursor.[12,25−36] Numerous carrying polymers were used, including poly(vinylpyrrolidone) (PVP),[25,30,31,33] poly(vinyl alcohol),[12,28,35] poly(ethylene oxide),[33] or Pluronic F127.[12,26,32] When combining the sol−gel method with electrospinning, there is no need of a carrying polymer.[26,27,29,36]

Because TEOS is well soluble in H_2O, the H_2O-based solutions were used for sol−gel solution that undergoes pregelation (aging) of TEOS, which is followed by the main spinning process.[26,27,29,36] The alcohol-based spun solutions usually contain ethanol and methanol with other solvents like dimethylformamide[36] or dimethyl sulfoxide.[33] The polymeric reaction of TEOS is driven and stabilized by hydrochloric acid (HCl),[26,33,37] acetic acid,[25,34,36] or H_3PO_4.[30] The specific surface area of fibers can be further increased by addition of a surfactant into the spun solution, for example, Pluronic F127.[26,29,35] Finally, the spun solutions undergo electrostatic

Received: June 12, 2017
Accepted: August 14, 2017
Published: August 28, 2017

DOI: 10.1021/acsomega.7b00770
ACS Omega 2017, 2, 5052−5059

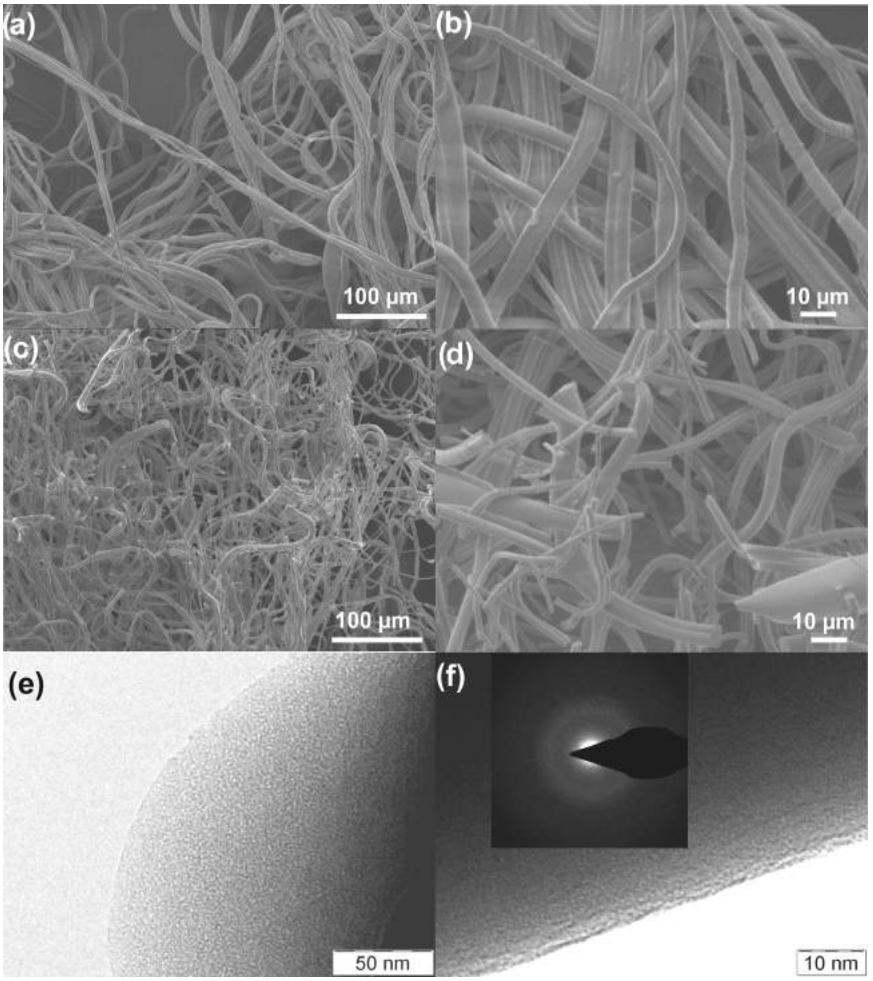

Figure 1. SEM images of (a, b) as-spun fibers and (c, d) calcined SiO_2 fibers, (e, f) TEM images of calcined SiO_2 fibers. All fibers are prepared from solution TEOS/PVP 1:1. The inset in (f) shows the selected-area diffraction pattern revealing an amorphous material.

spinning using conditions that strongly depend on the design of the spinning tool. Most typically, the voltage and the distance between electrodes are in the range of dozens of kilovolts and 5−20 cm, respectively.

The literature on electrospun SiO_2 fibers reports the mean fiber diameter to be in the range of 100−500 nm. Until now, there has been no other technique capable of production of fibers with such small diameters. However, the available literature provides only limited data on the detailed textural properties. Out of the eight papers available on electrospun SiO_2 fibers,[12,26,27,30,32,38−40] five of them contain textural properties. Data from these papers are summarized in Table S1 in the Supporting information. Specific surface areas span from 120 to 506 m^2/g and porosity of the fibers cover a broad range of microporosity and mesoporosity depending on the condition of spinning and composition of the solution. However, electrospinning has also some disadvantages. From the handling point of view, the most serious problem is the electrostatic charge of electrospun fibers that causes difficulties for all kinds of mechanical handling. In addition, some spinning solutions also contain HCl, which causes a corrosion of the production facility. On the basis of the recent literature,[17,18] it seems that centrifugal spinning, where no electrostatic charge is involved, not only overcomes the disadvantages of electrospinning, but is also industrially upscalable, which is comparably difficult with electrospinning tools. In addition, the centrifugal spinning processes possess significantly higher yields (amount of fibers produced per unit of time) than those of conventional electrospinning processes. The pressurized spinning[19,20] further improves the positive yield figure.

To the best of authors' knowledge, so far only two synthetic papers were reported on the preparation of SiO_2 fibers by centrifugal spinning. In the first report, Jung et al.[23] utilized TMOS aqueous solution with a surfactant. Their mesoporous fibers reached a specific surface area of 605 m^2/g. This result is also listed in Table S1 along with electrospun SiO_2 fibers. In a recent paper by Ren et al.,[41] various nanofiber and microfiber SiO_2 assemblies were reported with fiber diameters well below 500 nm, which was previously exclusive only to electrospun fibers. These two papers, however, did not report any fiber application and used aqueous chlorine containing (corrosive and environmentally not favorable) spun solution. Thus, it is important to develop an advanced synthesis of SiO_2 fibers by centrifugal spinning and to exploit these fibers for applications.

In this work, we aim to contribute to this development. We present several new features: new spun solution without any chlorine agents, an optimized centrifugal spinning technique (industrially already exploited) yielding mesoporous SiO_2 fibers with excellent textural properties, and excellent results of the H_2O adsorption.

DOI: 10.1021/acsomega.7b00770
ACS Omega 2017, 2, 5052−5059

RESULTS AND DISCUSSION

Morphological and Structural Analysis of Fibers. Figure 1 shows scanning electron microscopy (SEM) and transmission electron microscopy (TEM) images of the as-spun and calcined SiO_2 fibers. As one can see, the fiber structure of the as-spun fibers was preserved after calcination. However, the integrity of the as-spun fibers was not preserved after calcination due to the volume contraction and gravimetric loss based on the burn-out of the carbonaceous compounds from the as-spun fibers (for thermal gravimetric results, see Figure S1 in the Supporting information). In other words, the fibers get shorter in length and smaller in diameter through the calcination process. The fibers are completely amorphous in nature, as evident from TEM images and the selected-area diffraction pattern in Figure 1f, and further corroborated by X-ray diffraction (XRD) measurements (see Figure S2). This is in line with the literature that reports crystallization of amorphous SiO_2 to quartz SiO_2 at as high a temperature as 1200 °C.[33]

The diameters of as-spun and calcined SiO_2 fibers are shown in Figure 2 for different TEOS/PVP ratios. All fibers were calcined at 500 °C for 6 h (as in Figure 1). Apparently, there is no clear trend of the increasing TEOS content on fiber diameters. In general, the diameter of the as-spun fibers is influenced by numerous factors, such as the type and the shape of spinnerette[1] and composition and viscosity of the solution.[42−45] However, according to the authors experience with the SiO_2 fiber production process, the temperature and relative humidity (RH) of the atmosphere in the spinning chamber influences the properties and quality of the prepared fibers. However, for the fiber synthesis presented here, the humidity and temperature of the spinning chamber were controlled and stable (30% RH and 35 °C). Therefore, the most important parameter influencing the fiber diameter within this work remains the absolute amount of TEOS in the precursor fibers. The largest diameter was observed in the case of TEOS/PVP 1.5:1 solution (which has 14.25 g of TEOS and 9.5 g of PVP in 100 g of the whole solution). Apparently, this diameter variation is due to the viscoelastic properties of the solution (influenced by the TEOS absolute amount) that for the given and constant size of nozzles within the spinnerette and the constant rotation speed influence the solution flow through the nozzles and the resulting diameter of withdrawn fibers. Interestingly, the measured dynamic viscosities of all four solutions lie in a relatively narrow range between 290 and 315 mPa s, provided that solutions based on TEOS/PVP 2:1 are most viscous from all solutions. According to Figure 2, for the given setup even a small viscosity difference influences strongly the diameter of as-spun as well as calcined SiO_2 fibers. It should be emphasized at this point that the fiber diameter is solely a consequence of the solution composition and the used setup (Figure 5). It cannot be influenced otherwise by any other process condition. It should also be noted that some as-spun fibers might have smaller diameters than those of calcined fibers (as apparent from the overlap of scatter bars in Figure 2). It is a natural feature of fiber production that fibers have a scattered distribution in fiber diameters. What is most important is that the mean of the fiber diameter is significantly lower for calcined fibers.

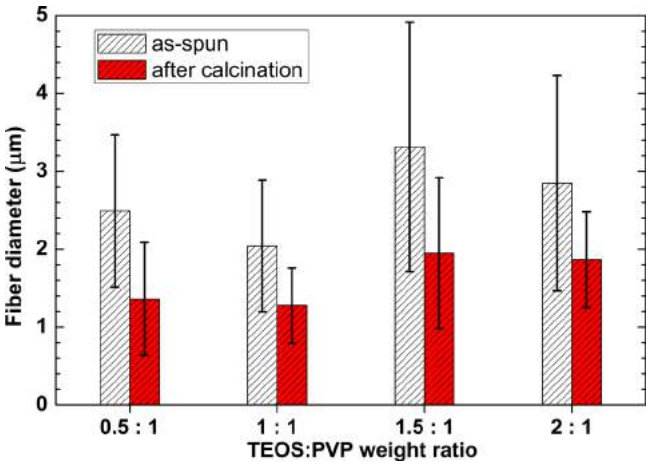

Figure 2. Diameter of as-spun and calcined SiO_2 fibers for different TEOS/PVP ratios.

Another important aspect of the inorganic fiber production, especially in terms of the costs, is the calcination yield. The calcination yield for fibers was calculated as a ratio of the mass of calcined SiO_2 fibers and the mass of as-spun fibers × 100%. It resulted into 8, 14, 17, and 25 wt % for fibers made out of solutions with increasing TEOS content. This is in line with expectation that the higher the TEOS content in the solution, the higher the gravimetric yield in terms of residual mass compared to the mass of as-spun fibers.

Textural Properties. Within preliminary experiments, the as-spun fibers were calcined at several different temperatures (450, 475, 500, 550, 600, and 650 °C). A successful calcination was considered as such a treatment that led to a snow-white 3D fiber network (without any apparent carbonaceous residues) after 6 h of soaking at the given temperature. The lowest temperatures (450 and 475 °C) resulted in gray fibers (which remained gray even for an extensive calcination time of 24 h). Temperatures from 500 °C (and higher) with soaking time of 6 h always led to the desired white product, SiO_2 fibers

Table 1 provides an overview of textural properties of SiO_2 fibers produced from all four solutions upon calcination of as-spun fibers at 500 °C for 6 h. For reference, textural properties of selected benchmark silicagel were analyzed too. The textural properties of all materials were derived from N_2 adsorption isotherms measured at the temperature of liquid nitrogen (isotherms are shown in Figures S3 and S4). The Brunauer−

Table 1. Summary of Textural Properties of the Samples[a]

sample	S_{BET} (m^2/g)	S_{ext} (m^2/g)	V_p (cm^3/g)	V_{micro} (cm^3/g)	D_p (nm)
TEOS/PVP 0.5:1	506 ± 1	32	0.326	0.020	2−7
TEOS/PVP 1:1	824 ± 3	65	0.547	0.011	2−10
TEOS/PVP 1.5:1	364 ± 1	18	0.191	0.069	1.5; 2−5
TEOS/PVP 2:1	424 ± 1	13	0.175	0.141	1.2; 1.55
reference silicagel	557 ± 1	14	0.640	0.000	4−17

[a]The specific surface (S_{BET}), external surface area (S_{ext}), total volume of the pores (V_p), volume of the micropores (V_{micro}), and porosity character.

DOI: 10.1021/acsomega.7b00770
ACS Omega 2017, 2, 5052−5059

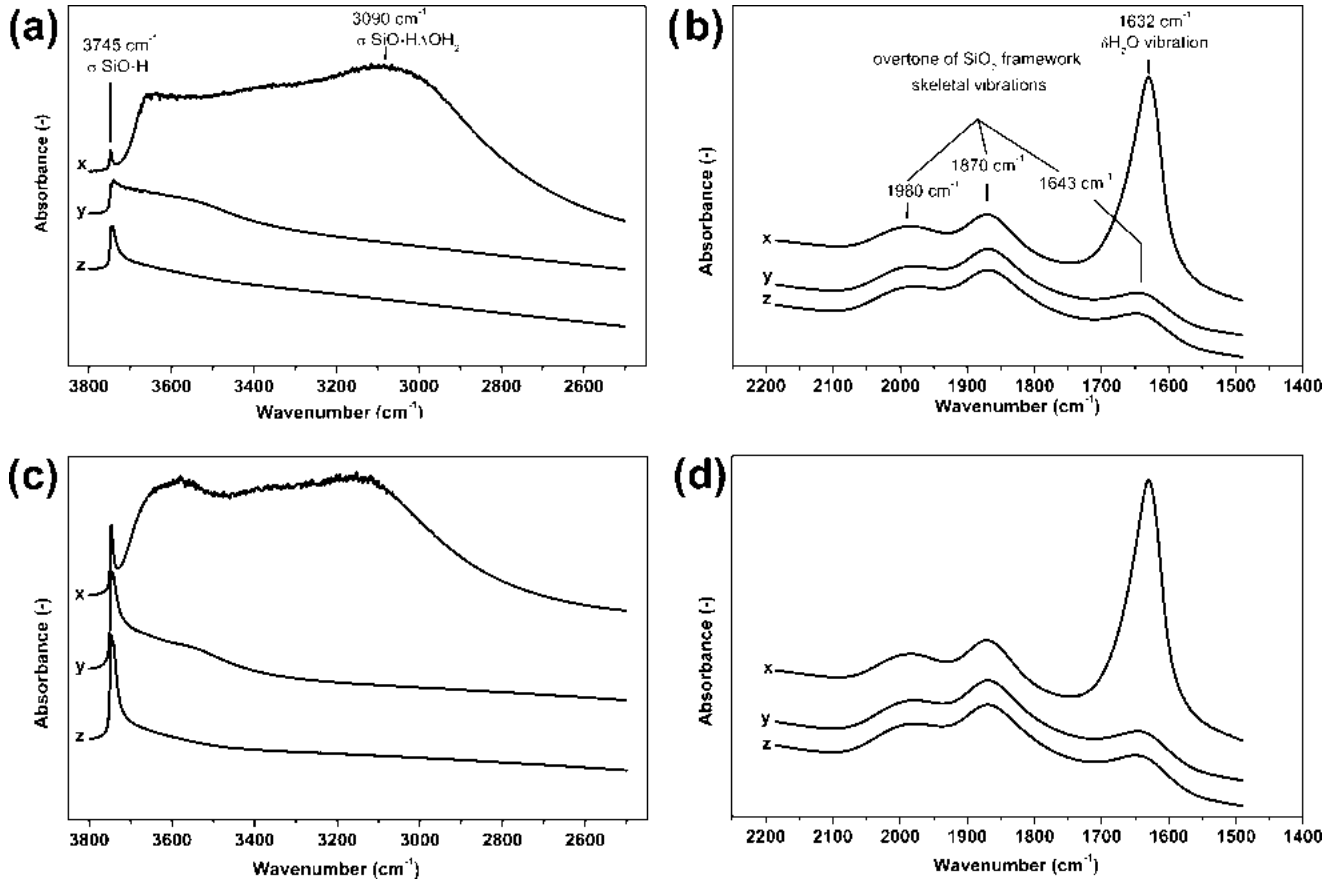

Figure 3. FTIR spectra of prepared TEOS/PVP 1:1 SiO_2 fibers (a, b) and reference silicagel (c, d); x is the fresh sample, y is the sample degassed under vacuum at 200 °C for 10 h, z is the sample degassed under vacuum at 490 °C for 3 h.

Emmett−Teller (BET) analysis showed that the highest total specific surface area and the external surface area (S_{BET} = 824 m^2/g and S_{ext} = 65 m^2/g) of the fibers was obtained in the case of TEOS/PVP 1:1 solution. This solution results also in the smallest diameter of the fibers (as shown in Figure 2) in good agreement with the trends in the external surface area. These fibers have also the largest volume of pores (V_p = 0.547 cm^3/g), which is an essential parameter for an efficient adsorption performance. Fibers from the other solutions have specific surface areas of no more than 506 m^2/g and comparably smaller pore volumes (at most 0.326 cm^3/g), as further shown in Table 1.

Interestingly, the TEOS/PVP ratio strongly influences the porosity character of the fibers. Although fibers from the TEOS/PVP 0.5:1 and 1:1 solution exhibit very low volume of micropores, the fibers produced from the solutions with TEOS/PVP ratios larger than 1 have a distinct microporous character, as can be documented by pore size distribution histograms for all fibers displayed in Figure S5. According to the literature, the typical specific surface areas of SiO_2 fibers produced by electrospinning are in the range of 200−500 m^2/g.[27,30−32] A paper by Jung et al. reported SiO_2 fibers by centrifugal spinning, with a specific surface area of up to 605 m^2/g achieved due to addition of surface active compounds in the spinning solution.[23] It is evident that SiO_2 fibers produced from the solution with the TEOS/PVP ratio of 1:1 reported here exhibit superior S_{BET} and V_p compared with materials reported in the literature. On the basis of the textural characteristics of these fibers, the benchmark type of silicagel (Merck grade 10180) was selected for comparison of adsorption properties. Silicagel textural properties are summarized in Table 1, and the adsorption isotherm and pore size distribution histogram are displayed in Figures S4 and S6, respectively.

Fourier Transformed Infrared (FTIR) Spectroscopy Analyses. FTIR spectra of the fiber sample (TEOS/PVP 1:1) and reference silicagel are presented in Figure 3. The vibration of silanol groups of fresh and degassed samples are very similar (Figure 3a,c). Both fresh samples (spectra x) exhibit intense bands at 1632 cm^{-1} assigned to the bending vibration of physically adsorbed H_2O molecules and the broad spectral feature in the range of 3700−2600 cm^{-1} caused by H-bonding of H_2O molecules on silanols. The subsequent evacuation at 200 °C led to H_2O desorption, evidenced by a disappearance of the band at 1632 cm^{-1} (a triplet of the band at 1980, 1870, and 1643 cm^{-1} visible in the spectra y and z depicted in Figure 4b,d is ascribed to the overtones of skeletal vibrations). The spectral region of O−H vibrations is dominated by the band at 3746 cm^{-1}, which is assigned to the terminal isolated or geminal silanols, whereas the low-frequency tail belongs to the H-bonded vicinal silanols.

On the basis of the relative comparison of spectra of both samples, it is evident that SiO_2 fibers contain higher population of H-bonded Si−OH groups. It can be caused by higher overall surface density of silanols or formation of silanol clusters or silanol nests. Calcination of the samples at 490 °C led to disappearance of the tail caused by dehydroxylation of H-

DOI: 10.1021/acsomega.7b00770
ACS Omega 2017, 2, 5052−5059

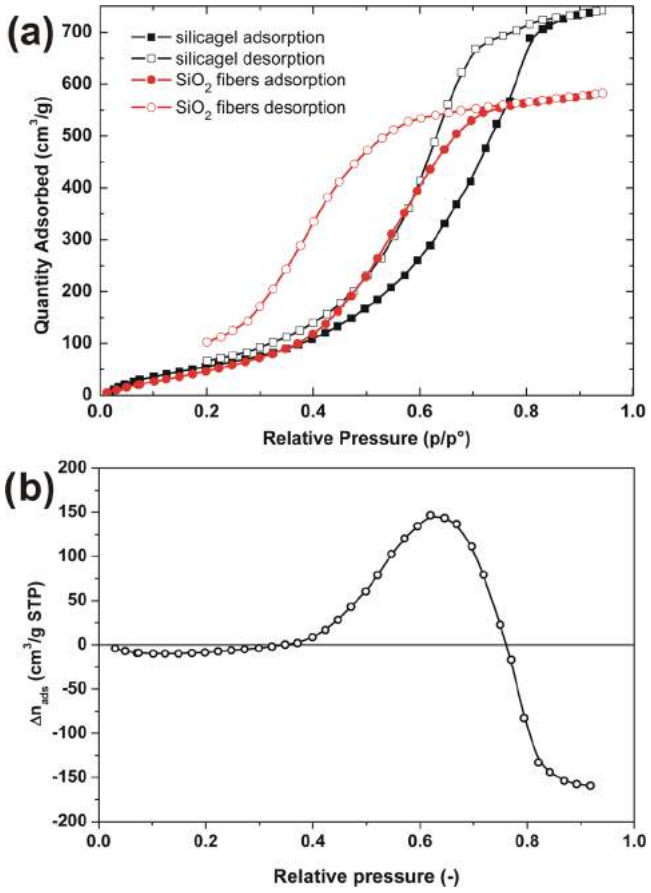

Figure 4. (a) Volumetric adsorption isotherms of H_2O vapors on SiO_2 fibers TEOS/PVP 1:1 and benchmark silicagel showing adsorption and desorption branches. Full points are the adsorption branch of isotherms and empty points are the desorption branch of isotherms; (b) difference isotherm obtained by subtraction of the adsorption branches of both isotherms depicted in (a) (SiO_2 fibers (TEOS/PVP 1:1), reference silicagel).

bonded vicinal silanols which exhibit low stability, as is generally accepted.

In general, a combination of the high specific surface area, hydrophilicity (density of surface silanol groups), and pore volume has a strong influence on the shape of the H_2O vapor adsorption isotherm and adsorption capacity.[46−48] On the basis of the differences in textural properties of SiO_2 fibers and reference silicagel, especially in the pore volume, the differences in the adsorption of H_2O could be expected.

All in all, considering the performance versus production cost figure (based on the favorable textural properties and the synthetic yield), SiO_2 fibers from solution TEOS/PVP 1:1 were selected as optimal for further testing by H_2O adsorption isotherms and FTIR.

H_2O Adsorption Performance. Figure 4a displays volumetric adsorption isotherms of the H_2O vapor on SiO_2 fibers (TEOS/PVP 1:1) and reference silicagel at 25 °C. Both isotherms belong to type IV concerning IUPAC classification with a similar character of the hysteresis loop, proving hydrophilicity of the surface and the fact that capillary condensation in mesopores is a dominant phenomenon at higher relative pressures of H_2O vapor.

From Figure 4b, it is evident that the adsorption performance at pressures below p/p_0 = 0.4 is almost the same for both materials. In the middle region (between relative pressures of 0.4 and 0.75), SiO_2 fibers overcome silicagel due to the narrower pore size distribution ranging from 2 to 8 nm (Figure S5b) compared to that of silicagel having pore size distribution between 2 and 20 nm (Figure S6). Above the relative pressure of 0.75, silicagel can adsorb more H_2O due to the presence of larger mesopores and a slightly higher total pore volume (see Table 1).

The reason for the strong prevalence of SiO_2 fibers in the range of medium humidities stems from the combination of their large surface area and steeper increase in the cumulative pore volume at smaller mesopores. The large area of the hydrophilic surface (see FTIR spectra of silanol vibration in Figure 3) implies a large number of silanol groups on the fiber surface through which H_2O molecules are adsorbed. In addition, the pore volume contributes to an additional H_2O uptake by capillary condensation taking place in the mesopores.

All in all, the results clearly show that SiO_2 fibers have the potential to be used advantageously for a broad range of applications, including desiccant wheel dehumidification systems[49] and solar-powered adsorption refrigeration.[50] Because of the above-mentioned reasons, this technique allows production of SiO_2 fibers on an industrial scale.

CONCLUSIONS

In this article, a novel type of 3D network of SiO_2 precursor fibers with a high surface area (≈824 m^2/g) and large pore volume was synthesized for the first time by centrifugal spinning from tailored spun solutions without toxic elements and surfactants. The optimized conditions for production of these fibers were found to be the following: utilization of solution with the TEOS/PVP ratio of 1:1 for centrifugal spinning, drying of as-produced fibers in air at controlled humidity (30% RH), and subsequent calcination in air at 500 °C for 6 h. On the basis of the textural characteristics of SiO_2 fibers, the benchmark type of silicagel was selected for comparison of the H_2O adsorption performance. From this comparison it is evident that SiO_2 fibers overcome silicagel in the humidity region between relative pressures of 0.4 and 0.75 due to a combination of their large surface areas and steeper increases in the cumulative pore volume in smaller mesopores. SiO_2 fibers are highly promising for production on an industrial scale.

EXPERIMENTAL DETAILS

Preparation of the Spun Solution. The spinning solution was prepared from two individual solutions. The first solution was prepared by mixing of 2 g of lactic acid, 4.75−19 g tetraethyl orthosilicate (TEOS), and 7 g of absolute ethanol. The second solution was prepared by dissolving 9.5 g of poly(vinylpyrrolidone) (PVP, M_w = 1 300 000 g/mol) in a mixture of 43.5−57.75 g of absolute ethanol and 19 g of *n*-butanol. The solution was stirred until all PVP was dissolved. Finally, both solutions were mixed together. In total, four different solutions with different TEOS/PVP ratios (0.5:1, 1:1, 1.5:1, and 2:1) were prepared. Viscosities of the as-prepared solutions were measured by a laboratory viscosimeter Maneko VP 1000.

Centrifugal Spinning Process. The recently developed centrifugal spinning technique was used for the synthesis of fibers with diameters on the microscale and sub-microscale.[17,18] A centrifugal spinning tool, Caltrop Spike Spinner CS18N,

DOI: 10.1021/acsomega.7b00770
ACS Omega 2017, 2, 5052−5059

developed and operated by the company Pardam Ltd. (Czech Republic) was used for the synthesis of the precursor 3D fiber network. The drawing of the tool is shown in Figure 5.

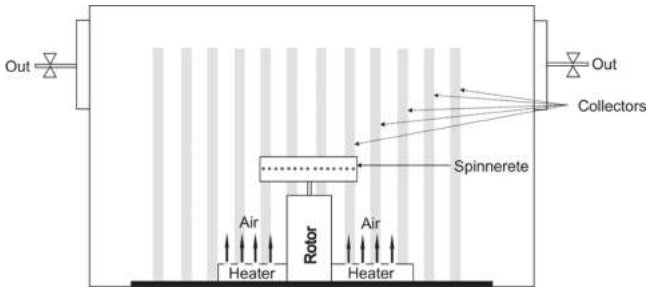

Figure 5. Schematic drawing of the centrifugal spinning setup.

To briefly outline the principle of centrifugal spinning, the solution is fed through many nozzles within the constantly rotating spinnerette (of a diameter of approximately 20 cm) at a constant flow rate. Centrifugal forces (due to rotation) spread out many fibers from the nozzles. Fibers are being dried from the solvents by an air flow (temperature and humidity controlled) while flying to the collectors, which are at a distance of approx. 50 cm from the geometrical center of the spinnerette. They are removed from collectors at regular periods (after sufficient amount of material has been collected, typically on the scale of 10−20 min) and submitted to calcination or analyses. This setup has several important advantages compared with electrospinning. The prepared fibers are in a "bulky" form, which allows for their easier handling. There is no nonwoven textile or aluminum foil needed for the process as a substrate, which has a positive impact on costs. The fibers are collected directly on the spacers. Finally, the as-prepared fibers do not possess an electrostatic charge, which also improves handling with fibers.

On the basis of preliminary experiments with solutions of different TEOS and PVP contents, the rotations of the spinnerette were set to 7000 rpm.

Calcination of the As-Spun Fibers. The prepared precursor fibers were calcined in a laboratory muffle oven. At first, all fiber batches were heated up to 300 °C (heating rate 0.8 °C/min) in ceramic crucibles and were maintained at this temperature for 1 h. Then, the temperature was increased to 500 °C (heating rate 10 °C/min) and maintained there for 6 h. Afterward, fibers were naturally cooled down to the room temperature.

For the purpose of adsorption properties comparison, a benchmark silicagel (high purity grade Merck grade 10180; Sigma-Aldrich) with similar textural properties was examined as well.

Morphological and Structural Analyses. The morphological characterization of as-spun as well as calcined SiO_2 fibers was carried out using a field-emission scanning electron microscope (JSM-7500F; JEOL) and a transmission electron microscope (JEM 2010F; JEOL). Diffraction analyses of the fibers were carried out using an X-ray diffractometer (XRD, D8 Advance; Bruker AXE), using Cu Kα radiation with secondary graphite monochromator and a Na(Tl)I scintillation detector.

BET Analysis. The textural properties (specific surface area and pore size distribution) of the SiO_2 fibers and reference silicagel were determined from the N_2 adsorption isotherms. The isotherms were acquired using an ASAP 2020 instrument (Micromeritics) and evaluated by MicroActive software (Micromeritics). Before the adsorption measurement, the fibers were carefully degassed to allow a quantitative removal of the preadsorbed H_2O. Starting at ambient temperature, the fibers were degassed at 110 °C (temperature ramp of 0.5 °C/min) until the residual pressure of 1 Pa was attained. After further heating at 110 °C for 1 h, the temperature was increased (temperature ramp of 1 °C/min) until a temperature of 200 °C was achieved. The SiO_2 fibers were degassed at this temperature under a turbomolecular pump vacuum for 8 h. This was done to avoid potential structural damage of the fibers due to surface tension effects and hydrothermal alternation. The specific surface area was calculated according to the BET method.[51] The mesopore and external surface area were determined by means of a *t*-plot using the Harkins−Jura equation for calculation of the adsorbed layer thickness; pore volume and pore size distribution were determined by the nonlocal density functional theory approach by using the "N_2 @ 77 K" model for cylindrical pores and oxide surface.

H_2O Adsorption Measurement. The adsorption isotherms of H_2O adsorbate on selected fibers and reference silicagel were also analyzed by the ASAP 2020 instrument (Micromeritics). The sample was activated in the same way as described above for N_2 adsorption measurement. H_2O adsorption isotherms were measured in the whole range of % RH at 25 °C using the tempered box equipped with Peltier elements and a Pt thermoprobe allowing temperature measurement and control in the range of −5 to 80 °C, with a precision of 0.1 °C.

Fourier Transformed Infrared (FTIR) Spectroscopy. For the FTIR experiments, the samples were pressed into self-supporting wafers with densities of ∼10 mg/cm^2 and placed into the IR cell for transmission measurement connected with the vacuum line (AABSPEC #2000A multimode system). The samples were in situ activated (outgassed) in dynamic vacuum (residual pressure < 10^{-4} mbar) for 10 h at 200 °C or 3 h at 490 °C (with a rate of temperature increase of 1 °C/min up to 127 °C; then, 30 min at this temperature and a subsequent increase of temperature with a rate of 5 °C/min up to the targeted temperature). Infrared spectra (32 scans) were collected at 25 °C (temperature was checked by the thermocouple embedded into the sample holder) with a resolution of 2 cm^{-1} on a Nicolet 6700 FTIR spectrometer equipped with an MCT/A cryodetector. IR spectra of the empty IR cell were taken as a background for each measured spectrum. For comparison and quantitative evaluation of individual measured samples, all spectra were normalized to unitary wafer surface density of 10.0 mg/cm^2 using integral intensity of skeletal overtones (2080−1740 cm^{-1}) as a benchmark.

■ ASSOCIATED CONTENT

Supporting Information

The Supporting Information is available free of charge on the ACS Publications website at DOI: 10.1021/acsomega.7b00770.

Thermogravimetry−differential thermal analysis; XRD pattern of calcined fibers; adsorption isotherm of N_2 (at temperature −196 °C); pore size distribution; data collected from the literature on textural properties of SiO_2 fibers (PDF)

DOI: 10.1021/acsomega.7b00770
ACS Omega 2017, 2, 5052−5059

AUTHOR INFORMATION

Corresponding Author

*E-mail: jan.macak@upce.cz. Phone: +420-466 037 401.

ORCID

Jan M. Macak: 0000-0001-7091-3022

Notes

The authors declare no competing financial interest.

ACKNOWLEDGMENTS

Financial support from Technology Agency of the Czech Republic (project TA04011557), Czech Science Foundation (project GACR P106/12/G015) and Ministry of Youth, Education, and Sports of the Czech Republic (project LM2015082) is gratefully acknowledged. We thank Prof. Petra Sulcova, Ph.D., for thermogravimetric analyses. We thank the company Pardam Ltd. for cooperation.

REFERENCES

(1) Teo, W. E.; Ramakrishna, S. A Review on Electrospinning Design and Nanofibre Assemblies. *Nanotechnology* **2006**, *17*, R89.

(2) Luo, C. J.; Stoyanov, S. D.; Stride, E.; Pelan, E.; Edirisinghe, M. Electrospinning versus Fibre Production Methods: From Specifics to Technological Convergence. *Chem. Soc. Rev.* **2012**, *41*, 4708−4735.

(3) Dalton, P. D.; Vaquette, C.; Farrugia, B. L.; Dargaville, T. R.; Brown, T. D.; Hutmacher, D. W. Electrospinning and Additive Manufacturing: Converging Technologies. *Biomater. Sci.* **2013**, *1*, 171−185.

(4) Demir, M. M.; Yilgor, I.; Yilgor, E.; Erman, B. Electrospinning of Polyurethane Fibers. *Polymer* **2002**, *43*, 3303−3309.

(5) Homaeigohar, S.; Koll, J.; Lilleodden, E. T.; Elbahri, M. The Solvent Induced Interfiber Adhesion and Its Influence on the Mechanical and Filtration Properties of Polyethersulfone Electrospun Nanofibrous Microfiltration Membranes. *Sep. Purif. Technol.* **2012**, *98*, 456−463.

(6) Su, C.; Shao, C.; Liu, Y. Electrospun Nanofibers of TiO_2/CdS Heteroarchitectures with Enhanced Photocatalytic Activity by Visible Light. *J. Colloid Interface Sci.* **2011**, *359*, 220−227.

(7) Yang, X.; Shao, C.; Liu, Y.; Mu, R.; Guan, H. Nanofibers of CeO_2 via an Electrospinning Technique. *Thin Solid Films* **2005**, *478*, 228−231.

(8) Xiang, H.; Long, Y.; Yu, X.; Zhang, X.; Zhao, N.; Xu, J. A Novel and Facile Method to Prepare Porous Hollow CuO and Cu Nanofibers Based on Electrospinning. *CrystEngComm* **2011**, *13*, 4856−4860.

(9) Kim, Y.-J.; Ahn, C. H.; Lee, M. B.; Choi, M.-S. Characteristics of Electrospun PVDF/SiO_2 Composite Nanofiber Membranes as Polymer Electrolyte. *Mater. Chem. Phys.* **2011**, *127*, 137−142.

(10) Wang, C.; Tong, Y.; Sun, Z.; Xin, Y.; Yan, E.; Huang, Z. Preparation of One-Dimensional TiO_2 Nanoparticles within Polymer Fiber Matrices by Electrospinning. *Mater. Lett.* **2007**, *61*, 5125−5128.

(11) Misha, S.; Mat, S.; Ruslan, M. H.; Sopian, K. Review of Solid/liquid Desiccant in the Drying Applications and Its Regeneration Methods. *Renewable Sustainable Energy Rev.* **2012**, *16*, 4686−4707.

(12) Saha, J.; De, G. Highly Ordered Cubic Mesoporous Electrospun SiO_2 Nanofibers. *Chem. Commun.* **2013**, *49*, 6322−6324.

(13) Wang, H.; Wu, Q.; Cao, D.; Lu, X.; Wang, J.; Leung, M. K. H.; Cheng, S.; Lu, L.; Niu, C. Synthesis of SnSb-Embedded Carbon-Silica Fibers via Electrospinning: Effect of TEOS on Structural Evolutions and Electrochemical Properties. *Mater. Today Energy* **2016**, *1*−*2*, 24−32.

(14) Wu, X.; Shi, Z.-q.; Wang, C.-y.; Jin, J. Nanostructured SiO_2/C Composites Prepared via Electrospinning and Their Electrochemical Properties for Lithium Ion Batteries. *J. Electroanal. Chem.* **2015**, *746*, 62−67.

(15) Doshi, J.; Reneker, D. H. Electrospinning Process and Applications of Electrospun Fibers. *J. Electrost.* **1995**, *35*, 151−160.

(16) Reneker, D. H.; Yarin, A. L. Electrospinning Jets and Polymer Nanofibers. *Polymer* **2008**, 2387−2425.

(17) Sarkar, K.; Gomez, C.; Zambrano, S.; Ramirez, M.; de Hoyos, E.; Vasquez, H.; Lozano, K. Electrospinning to Forcespinning. *Mater. Today* **2010**, *13*, 12−14.

(18) Edmondson, D.; Cooper, A.; Jana, S.; Wood, D.; Zhang, M. Centrifugal Electrospinning of Highly Aligned Polymer Nanofibers over a Large Area. *J. Mater. Chem.* **2012**, *22*, 18646−18652.

(19) Mahalingam, S.; Pierin, G.; Colombo, P.; Edirisinghe, M. Facile One-Pot Formation of Ceramic Fibres from Preceramic Polymers by Pressurised Gyration. *Ceram. Int.* **2015**, *41*, 6067−6073.

(20) Raimi-Abraham, B. T.; Mahalingam, S.; Edirisinghe, M.; Craig, D. Q. M. Generation of poly(N-Vinylpyrrolidone) Nanofibres Using Pressurised Gyration. *Mater. Sci. Eng., C* **2014**, *39*, 168−176.

(21) Ma, P. X.; Zhang, R. Synthetic Nano-Scale Fibrous Extracellular Matrix. *J. Biomed. Mater. Res.* **1999**, *46*, 60−72.

(22) Hong, Y.; Legge, R. L.; Zhang, S.; Chen, P. Effect of Amino Acid Sequence and pH on Nanofiber Formation of Self-Assembling Peptides EAK16-II and EAK16-IV. *Biomacromolecules* **2003**, *4*, 1433−1442.

(23) Jung, K. T.; Chu, Y.-H.; Haam, S.; Shul, Y. G. Synthesis of Mesoporous Silica Fiber Using Spinning Method. *J. Non-Cryst. Solids* **2002**, *298*, 193−201.

(24) Ellison, C. J.; Phatak, A.; Giles, D. W.; Macosko, C. W.; Bates, F. S. Melt Blown Nanofibers: Fiber Diameter Distributions and Onset of Fiber Breakup. *Polymer* **2007**, *48*, 3306−3316.

(25) Batool, S. S.; Imran, Z.; Israr-Qadir, M.; Jamil-Rana, S.; Usman, M.; Jamil, H.; Rafiq, M. A.; Hasan, M. M.; Nur, O.; Willander, M. Silica Nanofibers Based Impedance Type Humidity Detector Prepared on Glass Substrate. *Vacuum* **2013**, *87*, 1−6.

(26) He, H.; Wang, J.; Li, X.; Zhang, X.; Weng, W.; Han, G. Silica Nanofibers with Controlled Mesoporous Structure via Electrospinning: From Random to Orientated. *Mater. Lett.* **2013**, *94*, 100−103.

(27) Ma, Z.; Ji, H.; Teng, Y.; Dong, G.; Zhou, J.; Tan, D.; Qiu, J. Engineering and Optimization of Nano- and Mesoporous Silica Fibers Using Sol−gel and Electrospinning Techniques for Sorption of Heavy Metal Ions. *J. Colloid Interface Sci.* **2011**, *358*, 547−553.

(28) Shao, C.; Kim, H.-Y.; Gong, J.; Ding, B.; Lee, D.-R.; Park, S.-J. Fiber Mats of Poly(vinyl Alcohol)/silica Composite via Electrospinning. *Mater. Lett.* **2003**, *57*, 1579−1584.

(29) Yamaguchi, T.; Sakai, S.; Kawakami, K. Application of Silicate Electrospun Nanofibers for Cell Culture. *J. Sol−Gel Sci. Technol.* **2008**, *48*, 350−355.

(30) Wen, S.; Liu, L.; Zhang, L.; Chen, Q.; Zhang, L.; Fong, H. Hierarchical Electrospun SiO_2 Nanofibers Containing SiO_2 Nanoparticles with Controllable Surface-Roughness And/or Porosity. *Mater. Lett.* **2010**, *64*, 1517−1520.

(31) Wu, C.; Yuan, W.; Al-Deyab, S. S.; Zhang, K.-Q. Tuning Porous Silica Nanofibers by Colloid Electrospinning for Dye Adsorption. *Appl. Surf. Sci.* **2014**, *313*, 389−395.

(32) Wu, Y.-n.; Li, F.; Wu, Y.; Jia, W.; Hannam, P.; Qiao, J.; Li, G. Formation of Silica Nanofibers with Hierarchical Structure via Electrospinning. *Colloid Polym. Sci.* **2011**, *289*, 1253−1260.

(33) Liu, Y.; Sagi, S.; Chandrasekar, R.; Zhang, L.; Hedin, N. E.; Fong, H. Preparation and Characterization of Electrospun SiO_2 Nanofibers. *J. Nanosci. Nanotechnol.* **2008**, *8*, 1528−1536.

(34) Li, J.; Zhang, Y.; Zhong, X.; Yang, K.; Meng, J.; Cao, X. Single-Crystalline Nanowires of SiC Synthesized by Carbothermal Reduction of Electrospun PVP/TEOS Composite Fibres. *Nanotechnology* **2007**, *18*, No. 245606.

(35) Irani, M.; Keshtkar, A. R.; Moosavian, M. A. Removal of Cadmium from Aqueous Solution Using Mesoporous PVA/TEOS/APTES Composite Nanofiber Prepared by Sol−Gel/electrospinning. *Chem. Eng. J.* **2012**, *200*−*202*, 192−201.

(36) Choi, S.-S.; Lee, S. G.; Im, S. S.; Kim, S. H.; Joo, Y. L. Silica Nanofibers from Electrospinning/Sol−Gel Process. *J. Mater. Sci. Lett.* **2003**, *22*, 891−893.

DOI: 10.1021/acsomega.7b00770
ACS Omega 2017, 2, 5052−5059

(37) Feng, X.; Yang, G.; Xu, Q.; Hou, W.; Zhu, J.-J. Self-Assembly of polyaniline/Au Composites: From Nanotubes to Nanofibers. *Macromol. Rapid Commun.* **2006**, *27*, 31−36.
(38) Iimura, K.; Oi, T.; Suzuki, M.; Hirota, M. Preparation of Silica Fibers and Non-Woven Cloth by Electrospinning. *Adv. Powder Technol.* **2010**, *21*, 64−68.
(39) Katoch, A.; Kim, S. S. Synthesis of Hollow Silica Fibers with Porous Walls by Coaxial Electrospinning Method. *J. Am. Ceram. Soc.* **2012**, *95*, 553−556.
(40) Du, Q.; Wu, J.; Yang, H. Pt@Nb-TiO_2 Catalyst Membranes Fabricated by Electrospinning and Atomic Layer Deposition. *ACS Catal.* **2014**, *4*, 144−151.
(41) Ren, L.; Ozisik, R.; Kotha, S. P. Rapid and Efficient Fabrication of Multilevel Structured Silica Micro-/nanofibers by Centrifugal Jet Spinning. *J. Colloid Interface Sci.* **2014**, *425*, 136−142.
(42) Buchko, C. J.; Kozloff, K. M.; Martin, D. C. Surface Characterization of Porous, Biocompatible Protein Polymer Thin Films. *Biomaterials* **2001**, *22*, 1289−1300.
(43) Yang, Y.; Jia, Z.; Li, Q.; Guan, Z. Experimental Investigation of the Governing Parameters in the Electrospinning of Polyethylene Oxide Solution. *IEEE Trans. Dielectr. Electr. Insul.* **2006**, *13*, 580−585.
(44) Mit-uppatham, C.; Nithitanakul, M.; Supaphol, P. Ultrafine Electrospun Polyamide-6 Fibers: Effect of Solution Conditions on Morphology and Average Fiber Diameter. *Macromol. Chem. Phys.* **2004**, *205*, 2327−2338.
(45) Theron, S. A.; Zussman, E.; Yarin, A. L. Experimental Investigation of the Governing Parameters in the Electrospinning of Polymer Solutions. *Polymer* **2004**, *45*, 2017−2030.
(46) Zhuravlev, L. T. The Surface Chemistry of Amorphous Silica. Zhuravlev Model. *Colloids Surf., A* **2000**, *173*, 1−38.
(47) Nastaj, J.; Aleksandrzak, T. Adsorption Isotherms of Water, Propan-2-Ol, and Methylbenzene Vapors on Grade 03 Silica Gel, Sorbonorit 4 Activated Carbon, and HiSiv 3000 Zeolite. *J. Chem. Eng. Data* **2013**, *58*, 2629−2641.
(48) Oh, H.-T.; Lim, S.-J.; Kim, J. H.; Lee, C.-H. Adsorption Equilibria of Water Vapor on an Alumina/Zeolite 13X Composite and Silica Gel. *J. Chem. Eng. Data* **2017**, *62*, 804−811.
(49) Beccali, M.; Butera, F.; Guanella, R.; Adhikari, R. S. Simplified Models for the Performance Evaluation of Desiccant Wheel Dehumidification. *Int. J. Energy Res.* **2003**, *27*, 17−29.
(50) Khattab, N. M. A Novel Solar-Powered Adsorption Refrigeration Module. *Appl. Therm. Eng.* **2004**, *24*, 2747−2760.
(51) Brunauer, S.; Emmett, P. H.; Teller, E. Adsorption of Gases in Multimolecular Layers. *J. Am. Chem. Soc.* **1938**, *60*, 309−319.

DOI: 10.1021/acsomega.7b00770
ACS Omega 2017, 2, 5052−5059